Origin of Granular Capillarity Revealed by Particle-Based Simulations

Fengxian Fan,[1,2] Eric J. R. Parteli,[3] and Thorsten Pöschel[2]
[1]Shanghai Key Laboratory of Multiphase Flow and Heat Transfer in Power Engineering, University of Shanghai for Science and Technology, Jun Gong Road 516, 200093 Shanghai, China
[2]Institute for Multiscale Simulation, Friedrich-Alexander-Universität Erlangen-Nürnberg, Nägelsbachstraße 49b, 91052 Erlangen, Germany
[3]Department of Geosciences, University of Cologne, Pohligstraße 3, 50969 Cologne, Germany
(Received 14 June 2016; revised manuscript received 19 February 2017; published 23 May 2017)

When a thin tube is dipped into water, the water will ascend to a certain height, against the action of gravity. While this effect, termed capillarity, is well known, recent experiments have shown that agitated granular matter reveals a similar behavior. Namely, when a vertical tube is inserted into a container filled with granular material and is then set into vertical vibration, the particles rise up along the tube. In the present Letter, we investigate the effect of granular capillarity by means of numerical simulations and show that the effect is caused by convection of the granular material in the container. Moreover, we identify two regimes of behavior for the capillary height H_c^∞ depending on the tube-to-particle-diameter ratio, D/d. For large D/d, a scaling of H_c^∞ with the inverse of the tube diameter, which is reminiscent of liquids, is observed. However, when D/d decreases down to values smaller than a few particle sizes, a uniquely granular behavior is observed where H_c^∞ increases linearly with the tube diameter.

DOI: 10.1103/PhysRevLett.118.218001

Capillarity is one of the most fundamental effects of liquid behavior and has been investigated by many well-known scientists [1–6]. A review can be found in the book by de Gennes *et al.* [7]. Capillarity is a consequence of intermolecular attractive forces between the molecules of a liquid, causing surface tension, and between the molecules of the liquid and the tube. This explanation seems to prohibit the effect of capillarity in granular matter where the intermolecular forces between the molecules of the grains can be safely neglected as compared with gravitational and inertial forces at impact.

Nevertheless, recent experiments suggest that, under certain conditions, agitated granular matter reveals a similar behavior which is reminiscent of capillarity: when a narrow tube is inserted into a vertically vibrating container filled with glass beads, the particles rise inside the tube up to a certain height, just as liquid in a capillary tube [8]. The same is observed when the container is at rest but the tube is set into vertical vibration [9]. The described phenomenon can provide an efficient means for the handling and transportation of particulate materials in technical applications [9–12]. However, the physical mechanism which gives rise to this observation remains poorly understood. Although it is obvious that capillarity in fluids must be of a different nature than the phenomenon discussed here, we term it granular capillarity because of its striking phenomenological similarity to the corresponding effect in fluids.

In the present Letter we approach the problem by means of particle-based numerical simulations using the discrete element method; that is, we solve Newton's equations of motion for the particles in the system under the action of particle-particle and particle-wall forces and gravity (see Sec. I of the Supplemental Material [13], which includes Refs. [14–29]). In experiments under vacuum conditions it was shown that granular capillarity is not just an effect caused by the motion of interstitial air [9,11]; therefore, air flow does not need to be considered in the simulations.

We consider 116 900 noncohesive, frictional spherical particles of diameter $d = 0.6$ mm poured into the system shown in Fig. 1. This system consists of a rectangular container of width $w = 24$ mm in both lateral directions, in the center of which a cylindrical tube of length 1 m, inner diameter D (which will be varied in the simulations), and wall thickness 0.3 mm is vertically inserted. Specifically, we start the simulation by filling the inner volume of the container (including the inner volume of the cylinder in the container's center) with the particles placed at random positions, such as to obtain a solid fraction of approximately 25% throughout the simulation volume (which excludes the volume occupied by the cylinder). Thereafter we let the particles settle due to the action of gravity. Once the particles have been deposited, the tube is vibrated vertically with frequency f and amplitude A, while its bottom end is located at position z_b, which is a function of time t and is given by

$$z_b = A\sin(2\pi f t), \tag{1}$$

with $A = 8.6$ mm and $f = 12$ Hz, consistent with previous experiments [9,11,12]. Figure 1 shows a sequence of snapshots for $D = 8$ mm, or $D/d = 13.33$. The snapshots show two-dimensional cuts of the system along the axis

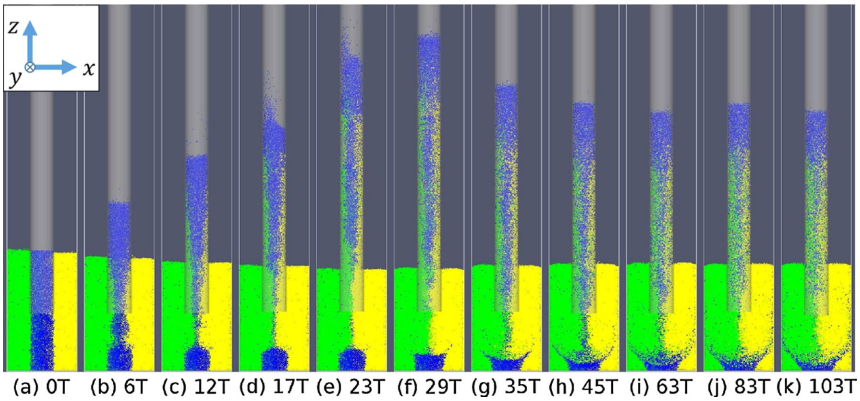

FIG. 1. Granular capillarity effect. When a narrow tube is dipped into granular material and vibrated vertically, the granular material rises inside the tube to reach a terminal vertical level. The snapshots (a)–(k) show the system at time, t, in units of the tube's oscillation period, $T = 1/f \approx 83$ ms. System parameters are provided in Sec. I of the Supplemental Material [13]. The tube-to-particle-diameter ratio is $D/d = 13.33$. Particles are color coded based on their initial positions at time $t = 0$, panel (a).

$x = 0$, while the particles are color coded according to their initial positions at $t = 0$.

The granular material inside the tube ascends until it reaches a stationary height at time $t \approx 50T$. The initial rise may be explained by a void-filling mechanism: Because of the upward motion of the tube, a void is left below the tube which is filled by particulate material from inside and outside the tube. The pressure originating from the granular system inside the tube is, however, limited by Janssen's law [30–32], whereas the pressure at the same vertical position but outside the tube is not limited (or at a much higher level due to the action of the container walls, respectively). Therefore, the void is filled preferentially by particles from outside the tube region, leading eventually to the observed rise of the granular system inside the tube. The process terminates when the filling level outside the tube has decayed to a level such that the pressure difference cancels [12]. The latter explanation is supported by another observation: In the simulation of Fig. 1, the initial filling heights inside and outside the tube are equal, $H_{\text{in}} = H_{\text{out}}$. Our simulations show, however, that this condition is unimportant for the asymptotic state, for given system characteristics. Specifically, the system converges always to the same value of $H_{\text{in}} - H_{\text{out}}$, namely H_c^{∞}, independently of the initial values of H_{in} and H_{out} (and including situations where, at $t = 0$, $H_{\text{in}} - H_{\text{out}} > H_c^{\infty}$), which is a behavior similar to the capillarity of liquids. This independence of the initial conditions agrees with experimental observations [10,11], but the origin of the reported behavior is explained for the first time in the present Letter, with the help of particle-based simulations.

To measure the capillary height, H_c, we divide the tube into cylindrical cells along its vertical axis, each of height $\delta z = 5d$, and compute the solid fraction of granular material at vertical position z,

$$\varphi(z) = N_p(z)[\pi d^3/6][(\pi D^2/4)\delta z]^{-1}, \qquad (2)$$

where $N_p(z)$ is the number of particles located in the cell at height z. We define H_{in} as the height of the cell above which the density drops below a threshold value of 10%. We find that choosing slightly larger or smaller thresholds lead to small differences in the granular column height of the order of a few grain diameters, while the value of 10% is taken as it is well below the lower bound of local packing fraction within the granular column during the tube vibrations (≈30%; see the Supplemental Material, Sec. II [13]).

The capillary height H_c is then defined as $H_{\text{in}} - H_{\text{out}}$, where H_{out} is the height of the particle layer in the tube's outer volume. Figure 2 shows H_c as a function of time for the simulation due to Fig. 1. Initially H_c increases at constant rate, thereafter reaches a maximum at $t \approx 25T$, and fluctuates around an average value $H_c^{\infty} \approx 47$ mm. The sinusoidal oscillation of the tube leaves a clear signature at H_c as a function of time. However, for $t \lesssim 20T$ the modulation of H_c follows $z_b(t)$ harmonically at small amplitude ($\approx A/2$), while for $t \gtrsim 20T$ H_c follows $z_b(t)$ subharmonically at much larger amplitude. Indeed, when the height of the granular column becomes large enough, the uppermost layers (which dictate H_c as explained above) eventually detach from the column and a zone of low solid fraction develops above the granular column. Although the

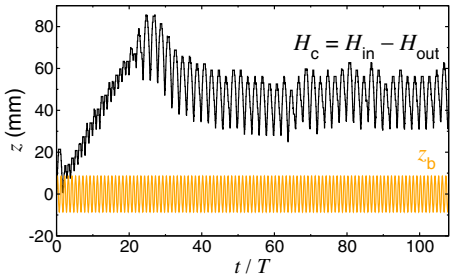

FIG. 2. Capillary height, H_c, as a function of time. z_b denotes the vertical position of the tube's lower end, see Eq. (1).

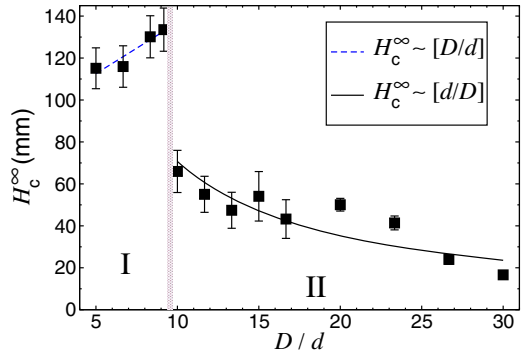

FIG. 3. Steady state capillary height, H_c^∞, as a function of D/d. Two different regimes are identified. For $D/d < 10$, we obtain a linear increase of H_c^∞ with D/d, while for larger D/d the scaling with d/D describes well the simulation data. Lines show best fits to the simulation data for both regimes.

detachment effect is related to the separation of the particles on top of the granular column [33], as also observed in our numerical simulations, the reason for the described change of the dynamics of the system at $t \approx 20T$ is not yet understood and is subject of current research. However, the referred behavior is clearly opposite to the Leidenfrost effect, where a dense granular column is supported by a rarified granular system [34–36]. Moreover, we find that the fluctuations of H_c observed in Fig. 2 are determined by the oscillations in H_{in}, as those in H_{out} are, comparatively, negligibly small.

Consider the steady state of the average capillary height, H_c^∞, in dependence on D/d (Fig. 3). From the data, we identify clearly two different regimes of behavior: For $D/d < 10$, H_c^∞ increases linearly with D/d (regime I), while for larger D/d the scaling reminiscent of liquids, $H_c^\infty \sim d/D$, describes very well the simulation results (regime II). The scaling $H_c^\infty \sim d/D$ was predicted by Ref. [12] based on a model which assumed balance of the gravitational potential energy of the granular column in the tube and the kinetic energy transferred to these particles due to collision with the grains below the bottom end of the tube as a result of the tube's vibration. Although we are not sure whether the assumptions of this model are entirely valid, for $D/d \gtrsim 10$, our simulation results confirm the prediction [12]. Note that this prediction has remained unchecked since so far neither long-term simulations producing the granular capillarity nor experiments with varying D/d have been performed.

We find that the frictional interactions between the particles and the walls of *both* the tube and the container are essential for producing the granular capillarity effect. To test the latter condition, we also performed simulations without the container's side walls, using periodic boundary conditions in the horizontal directions. In these simulations, the granular column within the tube does not rise (see the Supplemental Material, Sec. III [13]). However, since the container's width-to-particle-diameter ratio, w/d, plays an important role for the convective flow in agitated granular systems, we repeated the simulation of Fig. 1 but using a container with frictionless side walls (see the Supplemental Material, Sec. III [13]). In this simulation, we also observed no ascending of the granular column and thus no granular capillarity effect. The granular capillarity effect is thus not in essence a boundary effect, but occurs only if the container's walls are frictional.

But which role do the frictional walls at the container's sides play for granular capillarity? It has been shown in numerous previous studies that when a recipient filled with granular material is subjected to vertical vibrations, convection of the particulate system is produced, with particles near the frictional walls moving downwards and particles near the container's center being transported upwards [37–40]. This phenomenon is responsible, for instance, for the brazil nut effect, which causes segregation of binary mixtures with the bigger particles ending at the surface [41–43]. In the system investigated here, the convective motion is different as it is not the rectangular container but the vertical tube that vibrates. Specifically, the rising motion of the granular column is driven by the influx of particles entering the tube through its bottom end as they move laterally from the container towards the tube's central axis (see the Supplemental Material, Sec. IV [13]). It is this lateral flux, which is caused by the convective motion of the particulate system in the container, that provides the feeding mechanism for increasing the volume of granular material within the tube.

The conditions for granular convection have been studied by many authors before [38,44,45], and it is, thus, not our goal here to investigate details of the convective behavior as a function of system properties. Such behavior depends on several nondimensional quantities, including w/d, w/D, A/d, and $g/(Af^2)$, although we find that the presence of an abrupt transition between regimes I and II such as in Fig. 3 is robust with respect to these quantities. Instead of scrutinizing the dependence of convection characteristics on the system parameters, our goal here is to identify the origin of granular capillarity. As shown here for the first time, this origin is the granular convection: by suppressing convection, no granular capillarity occurs. To confirm that causality is not in the opposite direction, we repeated the simulations by "freezing" the particles within the tube at their initial positions, and noted that convection in the container still occurs (Supplemental Material, Sec. V [13]). This convection is induced by the system's vibrations and is not caused by the capillarity phenomenon.

Our simulations show that the abrupt transition between regimes I and II (Fig. 3) is consequence of a boundary effect on the dynamics of the granular column within the tube. To get a better understanding of these dynamics, we compute the time-volume-averaged vertical velocity $\langle v_z \rangle$ of the particles within the tube as a function of the radial position. This computation is performed by dividing the

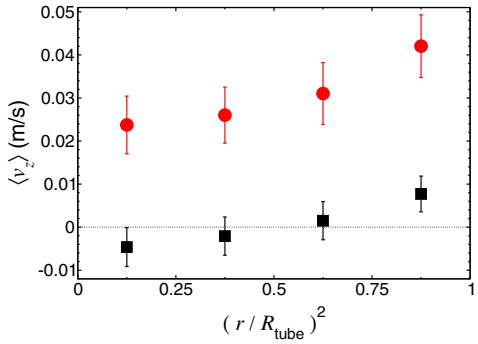

FIG. 4. Average vertical velocity $\langle v_z \rangle$ of the particles in the tube as a function of the squared nondimensional radial position, $(r/R_{\text{tube}})^2$. Circles denote results for the ascending phase ($t \lesssim 20T$), while squares correspond to the steady-state phase ($t \gtrsim 50T$). The dotted line indicates $\langle v_z \rangle = 0$.

inner volume of the tube in four cylindrical shells of equal volume and averaging the particle vertical velocity over all particles and over time within each shell.

Figure 4 shows the results of this computation for the simulation of Fig. 1 (regime II) both for the rising or ascending phase (circles)—that is, the phase where the granular column ascends along the tube—as well as for the steady-state phase (squares) where H_c fluctuates around H_c^∞. Because of shearing caused by frictional forces, $\langle v_z \rangle$ is larger for particles near the tube's inner wall than for those close to the tube's central axis, while in the steady-state phase, convection within the tube is observed. From Fig. 5, we see that particles moving near the tube's inner wall are those from the tube's outer volume, which are fed by the aforementioned lateral flux caused by convection in the container. Figure 5 shows the number fraction P_{out} of particles that, at $t = 0$, were in the outer volume of the tube in the simulation of Fig. 1, as a function of height and radial

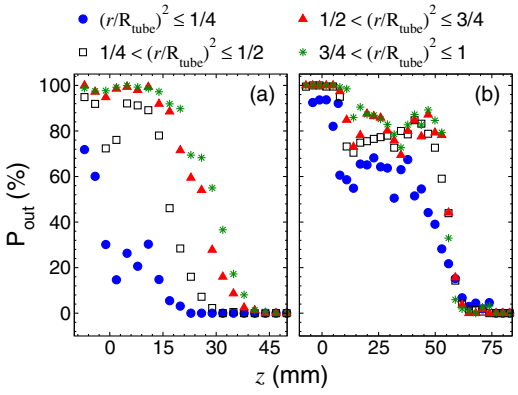

FIG. 5. Number fraction P_{out} of particles that were at the outer volume of the tube at $t = 0$. P_{out} is shown as a function of the vertical position z for different values of the radial position r. (a) and (b) refer to simulation results at $t = 10T$ and $t = 75T$, which correspond to snapshots in the ascending and steady-state regimes, respectively.

position within the tube, both for the rising [Fig. 5(a)] and steady-state [Fig. 5(b)] phases. P_{out} is defined as $N_{\text{out}}/(N_{\text{in}} + N_{\text{out}})$, where N_{in} and N_{out} denote the number of particles initially at the tube's inner and outer regions, respectively. That is, N_{in} corresponds to the blue particles with initial vertical positions $z_i(t = 0) > -A$ (where A is amplitude of vibration), while N_{out} is associated with all other particles. Clearly, P_{out} is larger near the wall than along the tube's central axis. In the steady state, this difference nearly vanishes due to convection.

The radial velocity gradient in Fig. 4, observed for all values of D/d in the regime II ($D/d \gtrsim 10$), does not occur for tube diameters smaller than about $10d$ (regime I). Our simulations show that, if the tube is very narrow, or $D \lesssim 10d$, interactions between particles near the inner wall with those along the central axis cause the whole granular column to move with nearly the same value of $\langle v_z \rangle$, independent of the particle's radial position. In regime I, the granular material flows irregularly, that is, stochastic perturbations become large and dominate the flow. Indeed, for $D/d \lesssim 3$ the flow of particles in the tube gets permanently blocked such that the measured value of H_c^∞ would be determined only by the (stochastic) time when the flow is blocked. Similar behavior is observed for granular pipe flow [46–64] with results reminiscent to what was observed here. Thus, while in regime II the dynamics of $H_c(t)$ are controlled by the shear-induced radial gradient in the vertical velocity shown in Fig. 4, in regime I $H_c(t)$ is governed by the stochastic interactions inherent to the jamming effect in granular flows through narrow tubes—it is this boundary effect that leads, thus, to the abrupt transition shown in Fig. 3. Therefore, these stochastic interactions, the convective mass flux in the system—which provides the particle influx through the tube's bottom end—as well as dissipation due to particle collisions and production due to working of the shear force on the sidewall surface through the slip velocity are important ingredients which should be added to the model of Ref. [12] for accurately predicting H_c^∞ as a function of system parameters.

We remark that the exact values of H_c^∞ and the critical D/d value separating regimes I and II certainly vary with the system's parameters. This dependence should inspire future work on systematic parameter variations with regard to the broad applicability of the granular capillarity phenomenon in particle handling and transportation in the industrial and technological sectors. However, here we have shown that this broad applicability, noted previously [9–12], is limited to systems where granular convection occurs. Granular capillarity does not occur if convection is suppressed from the granular system.

We thank the German Research Foundation for funding through the Cluster of "Excellence Engineering of Advanced Materials", the Collaborative Research Center 814 (Additive Manufacturing) and Grant No. RI2497/6-1,

the Shanghai Science and Technology Commission (13DZ2260900) and the National Natural Science Foundation of China (51206113, 51176128, 51576130) for financial support. We gratefully acknowledge the computing time granted by the John von Neumann Institute for Computing and provided on the supercomputer JUROPA at Jülich Supercomputing Centre. Support from Central Institute for Scientific Computing and Interdisciplinary Center for Functional Particle Systems at Friedrich-Alexander-University Erlangen-Nuremberg is gratefully acknowledged. F. F. thanks China Scholarship Council, which allowed her to spend a year at Friedrich-Alexander-University Erlangen-Nuremberg.

[1] R. Boyle, *New Experiments Physico-Mechanicall, Touching the Spring of the Air, and its Effects (Made, for the Most Part, in a New Pneumatical Engine) Written by Way of Letter to the Right Honorable Charles Lord Vicount of Dungarvan, Eldest Son to the Earl of Corke* (H. Hall, Oxford, 1660).
[2] R. Hooke, *An Attempt for the Explication of the Phænomena Observable in an Experiment Published by the Honourable Robert Boyle, Esq., in the XXXV Experiment of his Epistolical Discourse Touching the Aire* (Sam. Thomson, London, 1661).
[3] C. E. Gellert, Commentarii Academiae Scientiarum Imperialis Petropolitanae **12**, 243 (1740), http://www.biodiversitylibrary.org/item/38339#page/299/mode/1up.
[4] P. S. Laplace, *Traité de Mécanique Céleste*, Vol. 4 (Courcier, Paris, 1805).
[5] T. Young, Phil. Trans. R. Soc. London **95**, 65 (1805).
[6] C. F. Gauss, *Principia Generalia Theoriae Figurae Fluidorum in Statu Aequilibrii* (Dieterichianis, Göttingen, 1830).
[7] P.-G. de Gennes, F. Brochard-Wyart, and D. Quéré, *Capillarity and Wetting Phenomena: Drops, Bubbles, Pearls, Waves* (Springer, New York, 2004).
[8] W. Chen and R. Wei, Phys. Lett. A **244**, 389 (1998).
[9] C. Liu, P. Wu, and L. Wang, Soft Matter **9**, 4762 (2013).
[10] C. Liu, F. Zhang, P. Wu, and L. Wang, Powder Technol. **259**, 137 (2014).
[11] F. Zhang, L. Wang, C. Liu, and P. Wu, Acta Phys. Sin. **63**, 014501 (2014).
[12] Y. Liu and J. Zhao, Chin. Phys. B **24**, 034502 (2015).
[13] See Supplemental Material at http://link.aps.org/supplemental/10.1103/PhysRevLett.118.218001, which is organized as follows. In Section I, we provide the details of the numerical method employed in the numerical simulations. In Section II, we show the behavior of the vertical profile of the solid fraction within the vibrating tube. In Section III, we show that granular capillarity does not occur if the side frictional walls of the container are absent from the system. In Section IV, we show the velocity field of the particles for different tube sizes. In Section V, we show that convection still occurs if the particles within the tube are immobilized, thus confirming that convection in the container is caused by the system's vibrations without regard of capillarity.
[14] T. Pöschel and T. Schwager, *Computational Granular Dynamics* (Springer, Berlin Heidelberg, 2005).
[15] J. Schäfer, S. Dippel, and D. E. Wolf, J. Phys. I (France) **6**, 5 (1996).
[16] H. Kruggel-Emden, E. Simsek, S. Rickelt, S. Wirtz, and V. Scherer, Powder Technol. **171**, 157 (2007).
[17] H. Kruggel-Emden, S. Wirtz, and V. Scherer, Chem. Eng. Sci. **63**, 1523 (2008).
[18] N. V. Brilliantov, F. Spahn, J.-M. Hertzsch, and T. Pöschel, Phys. Rev. E **53**, 5382 (1996).
[19] P. A. Cundall and O. D. L. Strack, Geotechnique **29**, 47 (1979).
[20] T. Schwager and T. Pöschel, Phys. Rev. E **78**, 051304 (2008).
[21] T. Schwager and T. Pöschel, Phys. Rev. E **57**, 650 (1998).
[22] R. Ramírez, T. Pöschel, N. V. Brilliantov, and T. Schwager, Phys. Rev. E **60**, 4465 (1999).
[23] P. Müller and T. Pöschel, Phys. Rev. E **84**, 021302 (2011).
[24] C. H. Rycroft, A. V. Orpe, and A. Kudrolli, Phys. Rev. E **80**, 031305 (2009).
[25] E. J. R. Parteli, J. Schmidt, C. Blümel, K.-E. Wirth, W. Peukert, and T. Pöschel, Sci. Rep. **4**, 6227 (2014).
[26] J. Ai, J. F. Chen, J. M. Rotter, and J. Y. Ooi, Powder Technol. **206**, 269 (2011).
[27] E. J. R. Parteli, AIP Conf. Proc. **1542**, 185 (2013).
[28] E. J. R. Parteli and T. Pöschel, Powder Technol. **288**, 96 (2016).
[29] C. Kloss, C. Goniva, A. Hager, S. Amberger, and S. Pirker, Prog. Comput. Fluid Dyn. **12**, 140 (2012).
[30] P. Huber-Burnand, Ann. Phys. (Berlin) **92**, 316 (1829).
[31] G. H. L. Hagen, Ber. Akad. Wiss. Berlin **35**, 35 (1852).
[32] H. A. Janssen, Z. Ver. Dtsch. Ing. **39**, 1045 (1895).
[33] S. Luding, E. Clément, A. Blumen, J. Rajchenbach, and J. Duran, Phys. Rev. E **50**, 4113 (1994).
[34] P. Eshuis, K. van der Weele, D. van der Meer, and D. Lohse, Phys. Rev. Lett. **95**, 258001 (2005).
[35] N. Rivas, S. Luding, and A. R. Thornton, New J. Phys. **15**, 113043 (2013).
[36] C. R. K. Windows-Yule, N. Rivas, D. J. Parker, and A. R. Thornton, Phys. Rev. E **90**, 062205 (2014).
[37] H. J. van Gerner, M. A. van der Hoef, D. van der Meer, and K. van der Weele, Phys. Rev. E **76**, 051305 (2007).
[38] Y. Lan and A. D. Rosato, Phys. Fluids **9**, 3615 (1997).
[39] F. Zhang, L. Wang, C. Liu, P. Wu, and S. Zhan, Phys. Lett. A **378**, 1303 (2014).
[40] C. Zeilstra, J. G. Collignon, M. A. van der Hoef, N. G. Deen, and J. A. M. Kuipers, Powder Technol. **184**, 166 (2008).
[41] S. S. Hsiau and H. Y. Yu, Powder Technol. **93**, 83 (1997).
[42] T. Elperin and E. Golshtein, Physica A (Amsterdam) **247A**, 67 (1997).
[43] D. A. Huerta and J. C. Ruiz-Suarez, Phys. Rev. Lett. **92**, 114301 (2004).
[44] J. B. Knight, E. E. Ehrichs, V. Y. Kuperman, J. K. Flint, H. M. Jaeger, and S. R. Nagel, Phys. Rev. E **54**, 5726 (1996).
[45] E. L. Grossman, Phys. Rev. E **56**, 3290 (1997).
[46] T. Pöschel, J. Phys. I (France) **4**, 499 (1994).
[47] J. Lee and M. Leibig, J. Phys. I (France) **4**, 507 (1994).

[48] T. Schäfer and D. E. Wolf, in *Traffic and Granular Flow*, edited by D. Wolf, M. Schreckenberg, and A. Bachem (World Scientific, Singapore, 1996), pp. 311–315.
[49] T. Riethmüller, L. Schimansky-Geier, D. Rosenkranz, and T. Pöschel, J. Stat. Phys. **86**, 421 (1997).
[50] O. Moriyama, N. Kuroiwa, M. Matsushita, and H. Hayakawa, Phys. Rev. Lett. **80**, 2833 (1998).
[51] A. Valance and T. Le Pennec, Eur. Phys. J. B **5**, 223 (1998).
[52] J. L. Aider, N. Sommier, T. Raafat, and J. P. Hulin, Phys. Rev. E **59**, 778 (1999).
[53] D. E. Wolf, T. Scheffler, and J. Schäfer, Physica A (Amsterdam) **274A**, 171 (1999).
[54] W. Chen, M. Hou, K. Lu, Z. Jiang, and L. Lam, Phys. Rev. E **64**, 061305 (2001).
[55] Y. Bertho, F. Giorgiutti-Dauphiné, T. Raafat, E. J. Hinch, H. J. Herrmann, and J. P. Hulin, J. Fluid Mech. **459**, 317 (2002).
[56] T. Scheffler and D. E. Wolf, Granular Matter **4**, 103 (2002).
[57] Y. Bertho, F. Giorgiutti-Dauphiné, and J. P. Hulin, Phys. Fluids **15**, 3358 (2003).
[58] O. Moriyama, N. Kuroiwa, S. Tateda, T. Arai, A. Awazu, Y. Yamazaki, and M. Matsushita, Prog. Theor. Phys. Suppl. **150**, 136 (2003).
[59] I. Bratberg, F. Radjai, and A. Hansen, Phys. Rev. E **71**, 011301 (2005).
[60] J. Hadjigeorgiou, J. F. Lessard, and F. Mercier-Langevin, J. South Afr. Inst. Min. Metall. **105**, 809 (2005).
[61] J. Hadjigeorgiou and J. F. Lessard, Int. J. Rock Mech. Min. Sci. **44**, 820 (2007).
[62] S. Å. Ellingsen, K. S. Gjerden, M. Grøva, and A. Hansen, Phys. Rev. E **81**, 061302 (2010).
[63] A. Janda, I. Zuriguel, J. Bienzobas, A. Garcimartín, and D. Maza, AIP Conf. Proc. **1542**, 710 (2013).
[64] F. Verbücheln, E. J. R. Parteli, and T. Pöschel, Soft Matter **11**, 4295 (2015).